resubmitted to Phys. Rev. A November 24, 1999

Magneto-Optical Trapping of Chromium Atoms

C. C. Bradley,* J. J. McClelland,† W. R. Anderson,‡ and R. J. Celotta

Electron Physics Group

National Institute of Standards and Technology

Gaithersburg, MD 20899-8412

ABSTRACT

We have constructed a magneto-optical trap for chromium atoms. Using trapping light at 425 nm and two repumping lasers tuned to intercombination transitions, over 10^6 atoms were trapped and average densities of over 10^{16} m^{-3} were obtained. Non-exponential loss of atoms is observed at high densities indicating inelastic collisions between trapped atoms. Over a range of trapping conditions, the density-dependent trap loss rate constant β is extracted from fluorescence decay curves and found to have values in the range of 10^{-15} m^3s^{-1}, much larger than is observed in alkali traps.

PACS 32.80.Pj, 34.50.Rk

Magneto-optical traps (MOTs) are now a common tool for cooling and confining ultracold vapors of alkali, alkaline-earth, and metastable noble-gas atoms. Such atom traps allow new physics opportunities that range from the measurement of basic atomic properties like excited-state lifetimes and atom-atom interactions[1] to the observation of Bose-Einstein condensation in dilute gases[2] and the creation of coherent atom beams[3]. Given the wealth and diversity of the new physics emerging from these applications of the MOT, it is natural to consider the merits and challenges of trapping new atomic species. Our motivation for trapping chromium atoms originates from a desire to have a high-flux, mono-energetic atom source for extending studies of laser-focused atom deposition[4]. A second motivation exists in the possible production of quantum-degenerate Bose and Fermi gases with different isotopes of Cr. To this end chromium has also been trapped in a purely magnetic trap[5].

For the majority of atoms in the periodic table, including chromium, effective laser cooling and trapping is more difficult than it is for alkalis because of a lack of a closed optical-cycling transition. When these atoms are excited by absorption of a laser photon they can relax via one or more decay channels to non-resonant final states, thereby shutting down the laser cooling/trapping process.

The principal transition of chromium, between the $^7S_3$ ground state and the $^7P_4$ excited state, is resonantly excited with light having a vacuum wavelength of 425.55 nm (see Fig. 1). This is a strong $J \leftrightarrow J + 1$ transition with a spontaneous decay lifetime τ ($\tau = 1/\Gamma$) of 32 ns and a corresponding two-level saturation intensity I_S of 85 W/m^2. For ^{52}Cr, which constitutes 84 % of the natural isotopic abundace, there is no hyperfine structure. As Cr atoms are excited to the $^7P_4$ state, they occasionally decay to either the

$^5D_3$ or $^5D_4$ metastable states via an intercombination transition. The transition probability out of the saturated $^7S_3 \leftrightarrow {}^7P_4$ system is of the order 10^3 s^{-1}. Without some intervention, these "optical leaks" limit the resonant laser cooling and trapping interaction time to a few milliseconds.

To extend this interaction time, we optically repump the atoms from the metastable states back into the ground state by resonant excitation of the $^5D_4 \leftrightarrow {}^7P_3$ and the $^5D_3 \leftrightarrow {}^7P_3$ lines, at vacuum wavelengths of 653.97 nm and 663.18 nm, respectively. Like the "optical leaks" these are weak intercombination transitions. For example, the known transition probability from the $^7P_3$ to the $^5D_4$ state is 6.0×10^3 s^{-1}, much slower than the 0.315×10^8 s^{-1} probability for the $^7S_3 \leftrightarrow {}^7P_4$ transition[6]. Despite their weak transition probabilities, these repumping transitions are easily saturated with relatively small laser intensities, facilitating rapid return of the atoms to the laser cooling/trapping process. It should be noted that repumping via the $^7P_4$ excited state has also recently been used to successfully trap chromium atoms in a MOT[7].

As shown by the schematic in Fig. 2, our experimental set-up includes an ion-pumped vacuum chamber and a laser system consisting of two frequency-stabilized dye lasers and two single-frequency laser diodes. The dye lasers are used for slowing and trapping while the laser diodes provide the optical repumping frequencies. Each of the dye lasers produces up to 250 mW of light near 425 nm, using stilbene-3 laser dye, pumped with 4 W of all-lines, UV argon-ion laser light. In order to provide stable laser cooling and trapping, the dye laser wavelengths are locked to the principal Cr resonance transition using an atom-beam locking technique (discussed briefly below). As indicated in the figure, the output of one of the dye lasers is split up and appropriately polarized to

form the magneto-optical trap[8]. The output of a second dye laser is frequency-chirped and directed to counter-propagate with the atom beam, thereby slowing atoms so that they may be loaded into the MOT.

The trap is located in the center of a six-way cross vacuum chamber with typical operating pressure 3×10^{-6} Pa (2×10^{-8} Torr). To help form a MOT, a pair of current-carrying, water-cooled, copper-tube coils are wrapped around opposite 100 mm diameter arms of the vacuum chamber cross. These coils produce a spherical-quadrupole magnetic field that has its zero located near the center of the chamber and axial and radial gradients of 0.18 T/m and 0.09 T/m, respectively (for a coil current of 33 A). To cool and confine the atoms, three nearly-orthogonal retro-reflected laser beams, nominally Gaussian with 8 mm $1/e^2$ diameter, overlap with the magnetic field zero. The axial MOT laser beam (parallel to the magnetic field symmetry axis) is split off from the main laser beam, with the remaining light divided nearly equally for the two radial trap beams. For the work described in this paper, the axial beam was approximately a factor of three less intense than each of the radial trap beams. This ratio was chosen because it resulted in a nearly spherical cloud of trapped atoms.

We have two methods for supplying atoms to the trap. Our initial studies[9] were achieved by loading atoms into the MOT from a resistively heated Cr-plated filament located approximately 30 mm from the trapping region. Loading the MOT with such a source is attractive since it is so simple. The filaments are readily made by electroplating Cr out of a chromate solution onto tungsten wires[10]. Loading the MOT from the hot filaments facilitated our rapid initial exploration of chromium trapping, without the additional complication of producing and slowing an atomic beam. Unfortunately, as an

atom beam source for a MOT, the chromium filaments have several limitations: (i) they suffer from relatively poor atom flux stability, a result of Cr-plating irregularities, and (ii) they produce short trap lifetimes due to increased background gas densities from out-gassing generated by the high temperatures. Despite these problems, the filaments prove to be a very reliable and helpful diagnostic tool.

To provide a steadier source of slow atoms, we chirp-cool an atomic beam from a commercial high-temperature cell. In the cell, up to 20 g of solid Cr is contained in a zirconia ceramic crucible that is held at a temperature near 1900 K. A Cr beam emerges from a 1 mm diameter aperture in the cell. Collimation by a second aperture results in an atomic beam that is approximately 10 mm in diameter as it crosses through the center of the six-way cross, located 580 mm downstream from the Cr source. Atoms in this atomic beam are slowed by interaction with a counterpropagating, frequency-modulated laser beam from the second dye laser, referred to as the "slowing laser." The laser frequency is modulated by application of a sinusoidal voltage to its external scan input[11]. The amplitude, offset and frequency of the modulation are adjusted to maximize the number of atoms delivered to the MOT, as indicated by the trap fluorescence. For the data presented here, the frequency of the laser was modulated over a detuning range of −760 MHz to −175 MHz, using a sine wave frequency of 174 Hz. The slowing laser beam typically has a power of a few tens of milliwatts. It has a diameter of about 6 mm ($1/e^2$) at the chamber window and is focused on the oven aperture.

To provide stable trap loading conditions, drift of the slowing laser's frequency is eliminated via an electronic servo loop. This servo is a gated electronic integrator that detects and compensates for laser frequency drift during periodic interruptions of the

laser frequency modulation, when the laser is temporarily returned to the Cr resonance. For both of the dye lasers in this experiment, wavelength stabilization is achieved by splitting off a weak probe beam from the laser to be locked and by intersecting this probe with an atomic beam at right angles. Laser frequency drift is detected from spatial variations in the resulting fluorescence, facilitated by imaging the crossed beam fluorescence onto a split-photodiode[12].

For optical repumping of the trapped atoms, two ~1 mW laser beams from single-frequency commercial laser diodes are focused to approximately 1 mm $1/e^2$ diameter and aimed to overlap with the trapped atom cloud profile. The initial coarse frequency tuning of these lasers is accomplished by passing the laser beams through an iodine vapor cell and by comparison of observed laser absorption peaks with published tabulated spectra[13]. This gets each laser within ~100 MHz of the desired Cr resonance. Each laser frequency is then fine-adjusted to maximize the fluorescence in the Cr MOT. Once the optimal frequencies are obtained, the two laser diode frequencies are stabilized by an electronic servo, using a scanning-etalon lock technique[14]. The scanned etalon is itself stabilized by reference to a commercial, wavelength-stabilized, helium-neon laser.

The total number and density of trapped atoms in the MOT are estimated from the measured size and brightness of the atom cloud. This is done by imaging the atom cloud by its fluorescence onto a charge-coupled-device (CCD) camera and also onto a calibrated photodiode. From the camera images, we found that the atom cloud density distribution was approximately Gaussian and that the distribution width varied strongly with the MOT parameters.

We obtain an estimate of the total number of atoms N from the photodiode signal P via the equation $N = P/(\varepsilon R)$, where ε accounts for the light-to-signal conversion ratio and the light collection efficiency, and R gives the estimated average rate for spontaneous emission of photons per atom. We determine ε from transmission measurements on our collection optics, estimates of the acceptance solid angle, and our detector calibration factor. R is calculated from the expression $R = \frac{1}{2}\Gamma S/(1+S+4\Delta^2)$, where $S = I/(\eta I_S)$, I is the total trap laser beam intensity (all six beams combined), Δ is our measured trap laser detuning divided by Γ, and ηI_S is the increased saturation intensity appropriate to atoms in the MOT. For this estimate we take $\eta = 2.3$, a value obtained by averaging Clebsch-Gordan coefficients, assuming equal populations in all of the ground state magnetic spin states for atoms in the trap and considering the mixture of polarizations of the trap laser beams[15].

We estimate the average density of atoms n_{av} in the MOT by assuming that the cloud of atoms has an isotropic Gaussian distribution. We write the density as

$$n(r) = \frac{N}{\pi^{3/2} w^3} e^{-r^2/w^2}, \qquad (1)$$

where w is the $1/e$ radius of the cloud. The average density is then obtained by multiplying the probability of an atom being at a location r by the density at that location and integrating over all space:

$$n_{av} = \int \frac{n(r)}{N} n(r)\, dV = \frac{N}{\bar{V}}, \qquad (2)$$

where we define the effective volume $\bar{V} \equiv 2\sqrt{2}\pi^{3/2} w^3$.

The cloud radius w is extracted from measurements on the CCD images. Since these represent a two-dimensional projection of the three-dimensional cloud, they can be

used to obtain size information through determination of the half-maximum area A_{HM}, defined as the area of the image in which the intensity is greater than half the maximum. For a Gaussian distribution, the 1/*e* radius *w* is related to A_{HM} via

$$w = \left(\frac{A_{HM}}{\pi \ln 2} \right)^{1/2} . \qquad (3)$$

Combining eqs. (2) and (3) yields

$$n_{av} = \frac{0.204 N}{A_{HM}^{3/2}} . \qquad (4)$$

With the goal of maximizing the number of trapped atoms, we systematically varied trap parameters and recorded images and total fluorescence signals. By optimizing the MOT laser detuning and total power, the repumping laser frequency, and the MOT coil current, we obtained a maximum of over 10^6 atoms when loading atoms from the laser-slowed atom beam. This maximum was obtained by using a MOT laser detuning of –16 MHz (–3.2 Γ), a total trap laser intensity of 0.67 mW/mm^2 and an optimal MOT coil current of 33 A, corresponding to axial and radial magnetic field gradients of 0.18 T/m and 0.09 T/m, respectively[16].

The dependence of the number and average density of trapped atoms on MOT laser detuning and total trap intensity is shown by Figs. 3 and 4. For the data in Fig. 3, the MOT laser detuning was held at −16 MHz and the laser intensity was varied as shown. For the data in Fig. 4, the MOT laser intensity was held constant at 0.65 mW/mm^2 and the laser detuning was varied from –0.73 Γ to –5.0 Γ (–3.6 MHz to –25.0 MHz). The repumping lasers were tuned and locked at values that gave a maximum of trap fluorescence and trapped atom number. We found that the optimal frequencies for the repumping lasers did not need to be adjusted as the other trap parameters were varied.

By attenuating each of the laser diodes, we verified that there was sufficient laser intensity to saturate the trap fluorescence; the repumping action did not decrease for small reductions of each repumper laser intensity.

Our reported measurements of number and density have two sources of uncertainty. First, there is an overall scale factor uncertainty, which we estimate to be approximately ±30 % for the number of atoms and ±45 % for the density. For the number of atoms, this is dominated by the uncertainties in the spontaneous emission rate[15] and the fluorescence collection efficiency. For the density, there is an additional uncertainty introduced by our lack of knowledge of the exact density distribution. Second, there is an uncertainty associated with point-to-point random experimental fluctuations, drift, etc., that may have occurred during the course of measuring the data in Figs. 3 and 4. This we estimate as being approximately ±3 % of the measured value.

In order to understand the factors that limit the number of trapped atoms, we also measured the lifetime of atoms in the MOT by interrupting the trap loading and observing decay of the trap fluorescence. Decay curves were obtained by monitoring the fluorescence signal with a digital storage oscilloscope while the slowing laser beam was blocked by an electronically-controlled shutter. The oscilloscope was triggered by a logic signal that controlled the shutter. Using the storage oscilloscope, a recorded decay curve was obtained by averaging at least 8 actual trap load/decay cycles.

Two decay curves are shown as examples in Fig. 5. The data shown in Fig. 5(a) correspond to a trap distribution initially containing about 4×10^5 atoms with an average density of 5×10^{12} m^{-3}, obtained with a detuning of –3.2 Γ (–16 MHz) and total MOT intensity of 0.26 mW/mm^2. The data shown in Fig. 5(b) correspond to an initial trap

distribution with a factor of 10 less atoms but with a much higher initial average density of 2×10^{15} m^{-3}, obtained with a trap laser detuning of –0.7 Γ (–3.5 MHz) and intensity of 0.65 mW/mm^2. The time-dependent behavior for these two conditions is clearly different, with the higher density data showing an initial fast decay followed by a slower decrease, and the lower density data showing simply a slow decrease.

To determine the trapping lifetime, each of these data sets was fit with a decaying exponential. For the data in Fig. 5(a) a good fit to a single exponential with a lifetime of (0.4±0.04) s was found (shown by the solid line). To obtain a similar good fit for the data in Fig. 5(b) (shown by the solid line), we found it necessary to exclude data for times before 500 ms because of the initial fast decrease. Examining all data sets, we found that if data prior to 500 ms is excluded from the fit, a single exponential decay provides a good fit and a consistent lifetime across all data sets. This lifetime is consistent with background-gas-collision-limited lifetime given the base pressure of 3×10^{-6} Pa (2×10^{-8} Torr). We verified this by introducing a partial pressure of H_2 (the dominant background gas) and observing a linear increase in the loss rate.

The fast initial decay of Fig 5(b) is highly suggestive of a density-dependent trap loss. To investigate this, we consider our decay measurements as a function of intensity and detuning in the framework of a model with a collisional trap-loss rate constant β. We write the time derivative for the number of trapped atoms as

$$\frac{dN}{dt} = -\gamma N - \beta \int n^2 dV \,, \qquad (5)$$

where N and n are the number and density of atoms in the trap, respectively, γ is a constant that accounts for trap loss due to collisions of trapped atoms with background gas, and dV is a differential volume element. We simplify this model by assuming that

the shape of the atom density distribution is Gaussian and independent of time, allowing us to write $\int n^2 dV = N^2/\overline{V}$. In this case the time dependence of N has the analytic solution[17]

$$N(t) = \frac{N_0 \gamma e^{-\gamma t}}{\gamma + \frac{N_0 \beta}{\overline{V}}\left(1 - e^{-\gamma t}\right)}, \qquad (6)$$

where N_0 is the atom number at $t = 0$.

Eq. (6) can be used to extract the trap-loss rate constant β from the fluorescence decay data sets. Fixing the appropriate value of γ (as determined from the single-exponential fit to the data after 500 ms), the quantity $N_0\beta/\overline{V}$ can be obtained as a free parameter in a fit of eq. (6) to the full decay data. Using the value for N_0 obtained from fluorescence intensity measurements then permits the determination of β. For all measured decay curves, excellent fits to the decay over the entire time span were obtained in this manner. The fine line in Fig. 5(b) shows an example of such a fit.

In Figures 6 and 7, the rate constant β obtained in this manner is shown as a function of laser power (Fig. 6) and detuning (Fig. 7). Overall, β appears to depend relatively weakly on laser parameters, ranging in value from approximately 0.5×10^{-15} m^3 s^{-1} to 4×10^{-15} m^3 s^{-1}. Little variation is seen as a function of detuning, while a slight systematic increase as a function of laser intensity is observed for large intensities. These values for β have uncertainties, shown by the error bars in Figs. (6) and (7), that are estimated from the effect of the uncertainty in γ on the determination of β. Further, we estimate an overall scale factor uncertainty of ±40 %, which arises from the trap model approximations and the scale factor uncertainty for N_0.

The main conclusion from these fits to the decay data is that collisions between Cr atoms can explain the observed initial strong decay of the dense trapped samples and that this density dependent loss strongly limits the number of trapped atoms obtained in our conventional MOT[18]. Since collisional loss processes are generally very complex phenomena[19], it is difficult to attribute the losses to any one process without further experimental investigation. We can say, however, that the dependencies of β on the trap laser power and detuning are qualitatively consistent with what is observed for trapped alkali atoms, particularly in the so-called "radiative-escape" regime where collisional trap loss is dominated by energy transfer collisions of excited atoms with other trapped atoms. To further elucidate this possible explanation, the axes at the top of Figs. 6 and 7 show the excited state fraction for the given intensity and detuning. As can be seen, there is a general increase in β with increasing excited state fraction, consistent with radiative escape. However, β is evidently not a function of this parameter alone, and more complex processes are clearly also involved.

An intriguing result of these measurements is the large magnitude of β obtained for Cr as compared to what is seen in alkali MOTs. As an example, observed values of β for sodium in a MOT with comparable trapping parameters are of order 5×10^{-17} m^3 s^{-1}[20], a factor of about 20 smaller than values reported here. Given the increased internal complexity of multi-electron atoms like Cr, it is perhaps reasonable to expect such a large rate for exoergic trap-loss-producing collisions between atoms in a near-resonant optical trap. However a detailed theoretical analysis would have to be done to bear this expectation out.

The discovery of such a large density-dependent loss rate for chromium has significant implications for its future application in atom optical experiments. The results reported here strongly motivate more detailed experimental and theoretical study of chromium collisions. In addition, trapped Cr can be rapidly pumped into one or more metastable states, in order to study their collisional properties and/or to use these atoms for atom deposition and surface growth studies or other applications.

Acknowledgements

The authors wish to thank Paul Julienne, Carl Williams, Paul Lett, Steven Rolston, and William Phillips for useful discussions. We also wish to thank members of the Electron Physics Group for technical assistance and support. This work was supported by the Office of Technology Administration of the U.S. Department of Commerce.

References

*Present address: Dept. of Physics and Astronomy, Texas Christian University, Fort Worth, TX.

†Author to whom correspondence should be addressed. Electronic address: jabez.mcclelland@nist.gov

‡Present address: Lighthouse Inc., Charlottesville, VA.

1. J. Weiner, V.S. Bagnato, S. Zilio, P.S. Julienne, Rev. Mod. Phys. **71**, 1 (1999).

2. M. H. Anderson, J. R. Ensher, M. R. Matthews, C. E. Weiman, and E. A. Cornell, Science **269**, 198 (1995); C. C. Bradley, C. A. Sackett, J. J. Tollett, and R. G. Hulet, Phys. Rev. Lett. **75**, 1687 (1995); K. B. Davis, M.–O. Mewes, M. R. Andrews, N. J. van Druten, D. S. Durfee, D. M. Kurn, and W. Ketterle, Phys. Rev. Lett. **75**, 3969 (1995).

3. E. W. Hagley, L. Deng, M. Kozuma, J. Wen, K. Helmerson, S. L. Rolston, and W. D. Phillips, Science 283, 1706 (1999); W. Ketterle and H.-J. Miesner, Phys. Rev. A 56, 3291 (1997).

4. W. R. Anderson, C. C. Bradley, J. J. McClelland, and R. J. Celotta, Phys. Rev. A **59**, 2476 (1999); J. J. McCleland, R. E. Scholten, E. C. Palm, and R. J. Celotta, Science **262**, 877 (1993)

5. J. D. Weinstein, R. deCarvalho, J. Kim, D. Patterson, B. Friedrich, and J. M. Doyle, Phys. Rev. A **57**, R3173 (1998).

6. All transition probabilities for Cr are obtained from G. A. Martin, J. R. Fuhr, and W. L. Wiese, J. Phys. Chem. Ref. Data, **17**, supplement no. 3 (1988).

7. A. S. Bell, J. Stuhler, S. Locher, S. Hensler, J. Mlynek, and T. Pfau, Europhys. Lett. **45**, 156 (1999).

8. E. L. Raab, M. Prentiss, A. Cable, S. Chu, and D. E. Pritchard, Phys. Rev. Lett. **59**, 2631 (1987).

9. C. C. Bradley, W. R. Anderson, J. J. McClelland, and R J. Celotta, Bull. Am. Phys. Soc. **43**, 1291 (1998).

10. J. J. McClelland, J. Unguris, R. E. Scholten, and D. T. Pierce, J. Vac. Sci. Technol. A **11**, 2863 (1993).

11. In an ideal situation, a linear sawtooth ramp would be slightly more efficient for this modulation. However, we found that varying the waveform of the modulation did not significantly improve trap loading and tended to increase the probability of mode hops in the laser.

12. J. J. McClelland and M. H. Kelley, Phys. Rev. A **31**, 3704 (1985); W. Jitschin, Applied Physics B **33**, 7 (1984).

13. S. Gerstenkorn and P. Luc, *Atlas du spectre d'absorption de la molecule d'iode, 14800-20000 cm^{-1}* (*Centre national de la recherche scientifique*, Paris, 1978).

14. B. G. Lindsay, K. A. Smith, and F. B. Dunning, Rev. Sci. Instrum. **62**, 1656 (1991).

15. T. P. Dinneen, C. D. Wallace, K-Y. N. Tan, and P. L. Gould, Opt. Lett. **17**, 1708 (1992).

16. All values of detuning presented in this paper have an uncertainty of ±1 MHz, due to uncertainties in determining exact resonance with the atom. Laser intensity values are uncertain to ±10 % of the stated value, due to uncertainties in detector calibration and

beam diameter measurements. Unless otherwise specified, all quoted uncertainties are intended to be interpreted as one-standard deviation combined random and systematic errors.

17. M. Prentiss, A Cable, J. E. Bjorkholm, and S. Chu, Opt. Lett. **13**, 452 (1988).

18. A dark-spot MOT should help overcome this limitation. See W. Ketterle, K. B. Davis, M. A. Joffe, A. Martin, and D. E. Pritchard, Phys. Rev. Lett. **70**, 2253 (1993).

19. See, e.g., S. D. Gensemer, V. SanchezVillicana, K. Y. N. Tan, T. T. Grove, and P. L. Gould, Phys. Rev. A **56**, 4055 (1997).

20. L. Marcassa, K. Helmerson, A.M. Tuboy, D.M.B.P. Milori, S.R.Muniz, J. Flemming, S.C. Zilio, and V.S. Bagnato, J. Phys. B **29**, 3051 (1996).

Figure Captions

Figure 1. Energy level diagram for chromium, showing the principal laser cooling transition, the "optical leaks," and the repumping transitions.

Figure 2. Simplified schematic of the experiment. The output of a frequency-stable, ring dye laser (Dye 1), tuned between 0 to 25 MHz below the $^7S_3 \leftrightarrow {}^7P_4$ chromium resonance, is divided into three beams (two are shown) to form a magneto-optical trap (MOT). The retro-reflected laser beams intersect in the region of a spherical-quadrupole magnetic field produced by current-carrying coils (MC) located outside of the vacuum chamber (VC). The output of a second dye laser (Dye 2) is directed to counter-propagate with the atomic beam emerging from an 1900 K chromium cell (Cr) and is tuned below the atomic resonance and frequency-chirped in order to produce slow atoms for capture by the MOT. A shutter (S) is used to interrupt the slowing of atoms, allowing measurement of the lifetime of trapped atoms. Laser diodes (Diode 1 and Diode 2) are used to optically repump atoms that are lost from the trap by spontaneous decay to metastable ^5D states. The laser diode wavelengths are stabilized by an electronic servo, referenced to a frequency-stable Helium-Neon laser (He-Ne) via a scanning Fabry-Perot interferometer (S-FPI). Mirrors are indicated by M, and beamsplitters by BS.

Figure 3. Trap population N (filled circles) and average density n_{av} (open circles) as a function of total (six-beam) MOT laser intensity I, for a fixed laser detuning of $-3.2\ \Gamma$ (-16 MHz) from the atomic resonance. Trap population values and density values have overall scale factor uncertainties of ±30 % and ±45 %, respectively, and random uncertainties of ±3 %.

Figure 4. Trap population N (filled circles) and average density n_{av} (open circles) as a function of MOT laser detuning Δ, for a fixed total (six-beam) laser intensity of 0.65 mW/mm^2. Trap population values and density values have overall scale factor uncertainties of ±30 % and ±45 %, respectively, and random uncertainties of ±3 %.

Figure 5. Observed MOT fluorescence decay curves for two different sets of trapping parameters. Each set of data points was obtained by averaging 8 MOT loading/decay cycles. The curves shown with the data are obtained either by fitting a simple decaying exponential to the data for times after 0.5 s (the heavy lines) or by fitting a non-exponential decay model to the data (the fine line). This model includes trap loss due to collisions between trapped atoms. Density dependence of the trap population decay is demonstrated by comparison of the data in (a) and (b). For (a) simple exponential decay was observed for an initial average density of 5×10^{12} m^{-3}, while in (b) the trapped sample had an initial average atom density of 2×10^{15} m^{-3}, and strongly non-exponential decay is evident.

Figure 6. Density-dependent trap loss rate constant β as a function of total (six-beam) MOT laser intensity I, for a fixed laser detuning of $-3.2\ \Gamma$ (−16 MHz) from the atomic resonance, obtained from trap fluorescence decay curves. The top axis shows the effective excited state fraction for the given laser intensity and detuning. The vertical error bars indicate the range of β values that were obtained from fits to the decay curves, given the experimental uncertainty in the trap lifetime. In addition, there is an overall scale factor uncertainty of ±40 %.

Figure 7. Density-dependent trap loss rate constant β as a function of MOT laser detuning Δ, for a fixed total (six-beam) laser intensity of 0.65 mW/mm^2, obtained from

trap fluorescence decay curves. The top axis shows the effective excited state fraction for the given laser intensity and detuning. The vertical error bars indicate the range of β values that were obtained from fits to the decay curves, given the experimental uncertainty in the trap lifetime. In addition, there is an overall scale factor uncertainty of ±40 %.

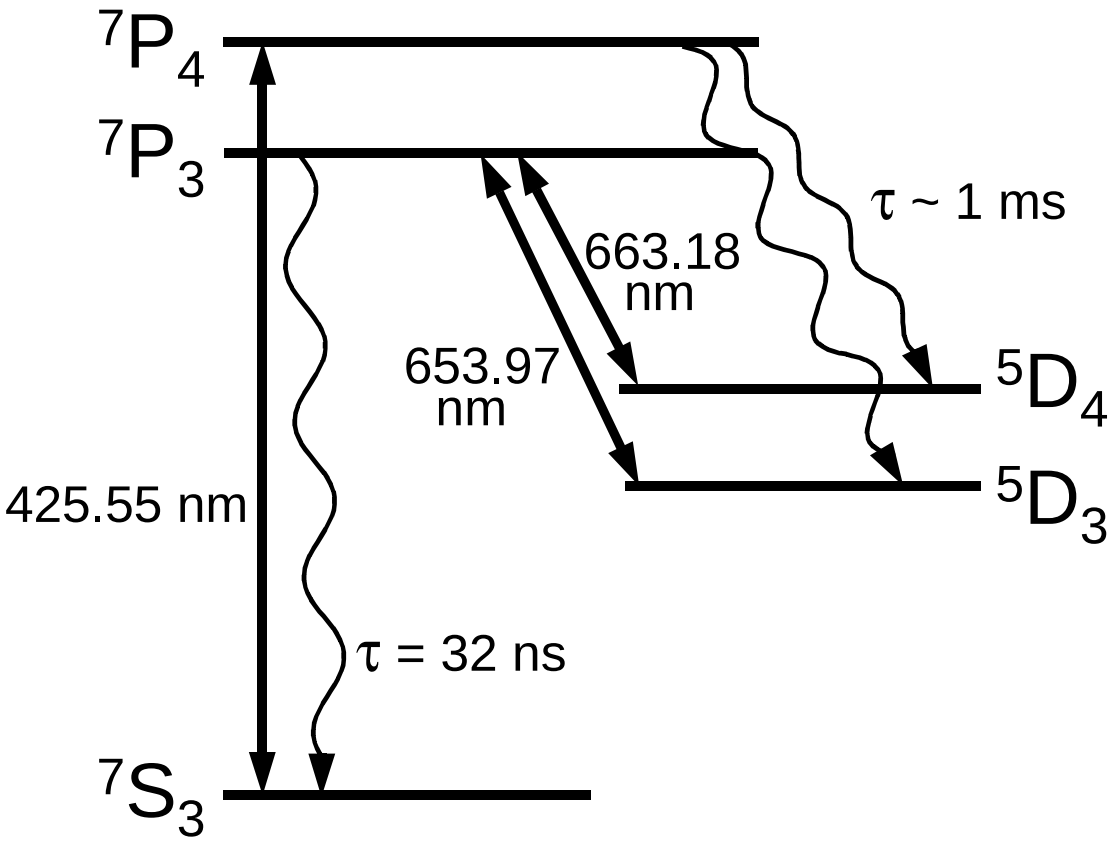

Figure 1. Energy level diagram for chromium, showing the principal laser cooling transition at 425.55 nm vacuum wavelength, the "optical leaks", and the repumping transitions at 653.97 nm and 663.18 nm.

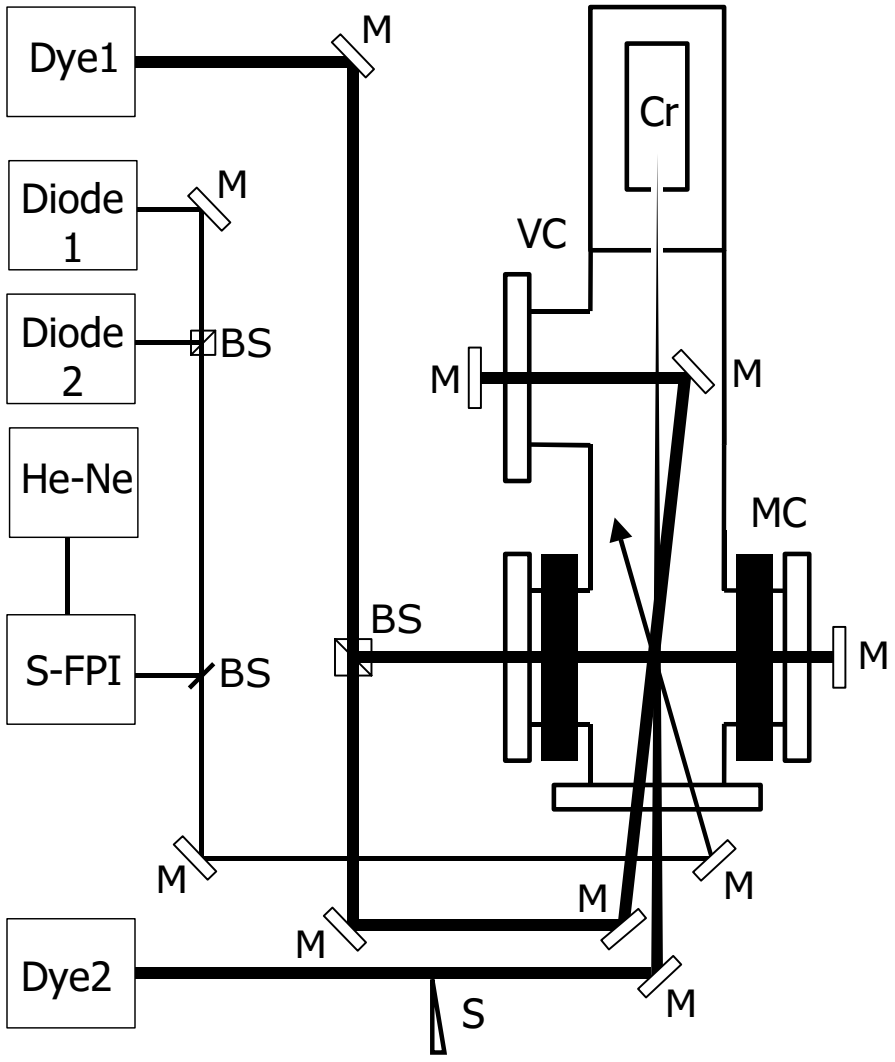

Figure 2. Simplified schematic of the experiment. The output of a frequency-stable, ring dye laser (Dye 1), tuned between 0 to 25 MHz below the $^7S_3 \leftrightarrow {}^7P_4$ chromium resonance, is divided into three beams (two are shown) to form a magneto-optical trap (MOT). The retro-reflected laser beams intersect in the region of a spherical-quadrupole magnetic field produced by current-carrying coils (MC) located outside of the vacuum chamber (VC). The output of a second dye laser (Dye 2) is directed to counter-propagate with the atomic beam emerging from an 1900 K chromium cell (Cr) and is tuned below the atomic resonance and frequency-chirped in order to produce slow atoms for capture by the MOT. A shutter (S) is used to interrupt the slowing of atoms, allowing measurement of the lifetime of trapped atoms. Laser diodes (Diode 1 and Diode 2) are used to optically repump atoms that are lost from the trap by spontaneous decay to metastable 5D states. The laser diode wavelengths are stabilized by an electronic servo, referenced to a frequency-stable Helium-Neon laser (He-Ne) via a scanning Fabry-Perot interferometer (S-FPI). Mirrors are indicated by M, and beamsplitters by BS.

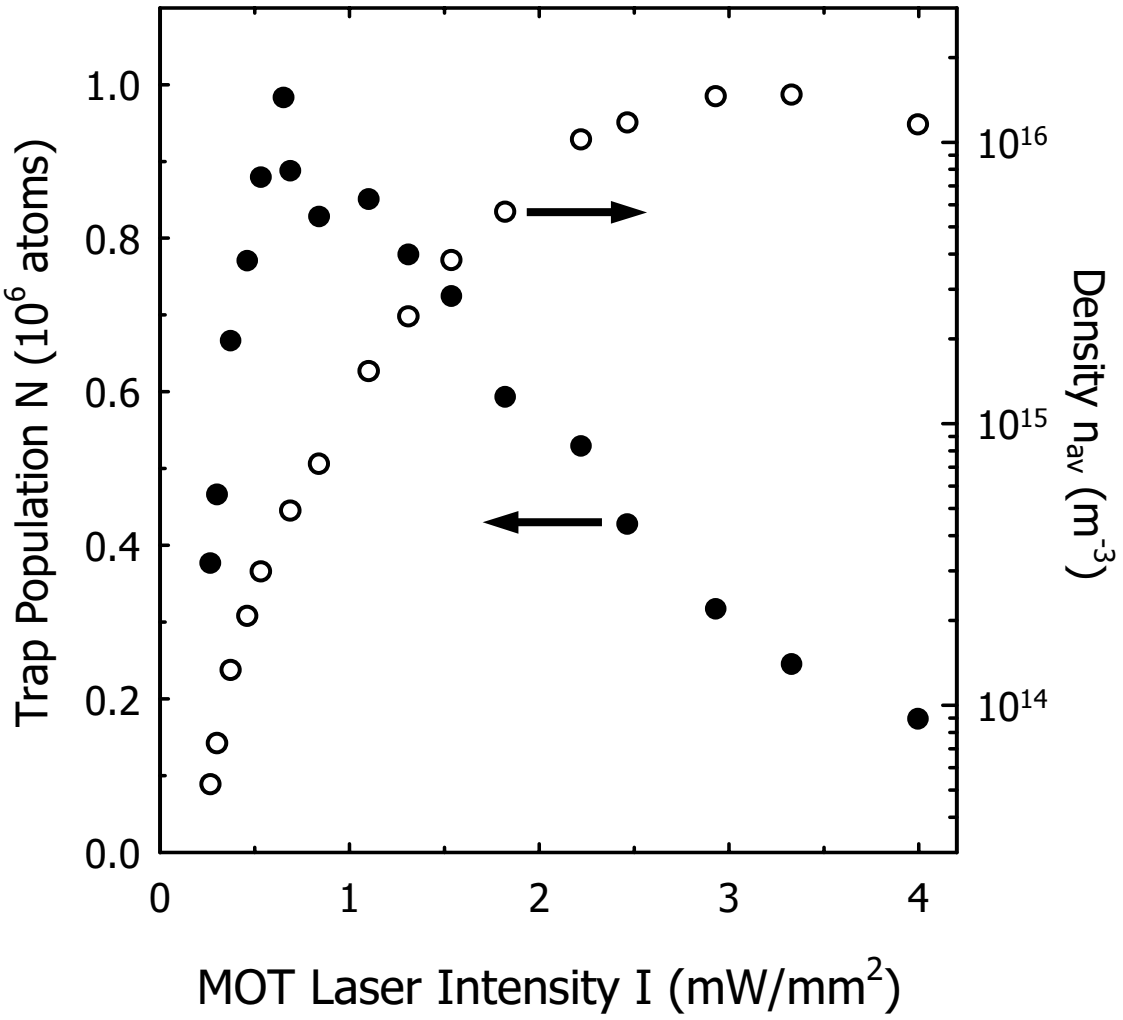

Figure 3. Trap population N (filled circles) and average density n_{av} (open circles) as a function of total (six-beam) MOT laser intensity I, for a fixed laser detuning of –3.2 Γ (–16 MHz) from the atomic resonance. Trap population values and density values have overall scale factor uncertainties of ±30 % and ±45 %, respectively, and random uncertainties of ±

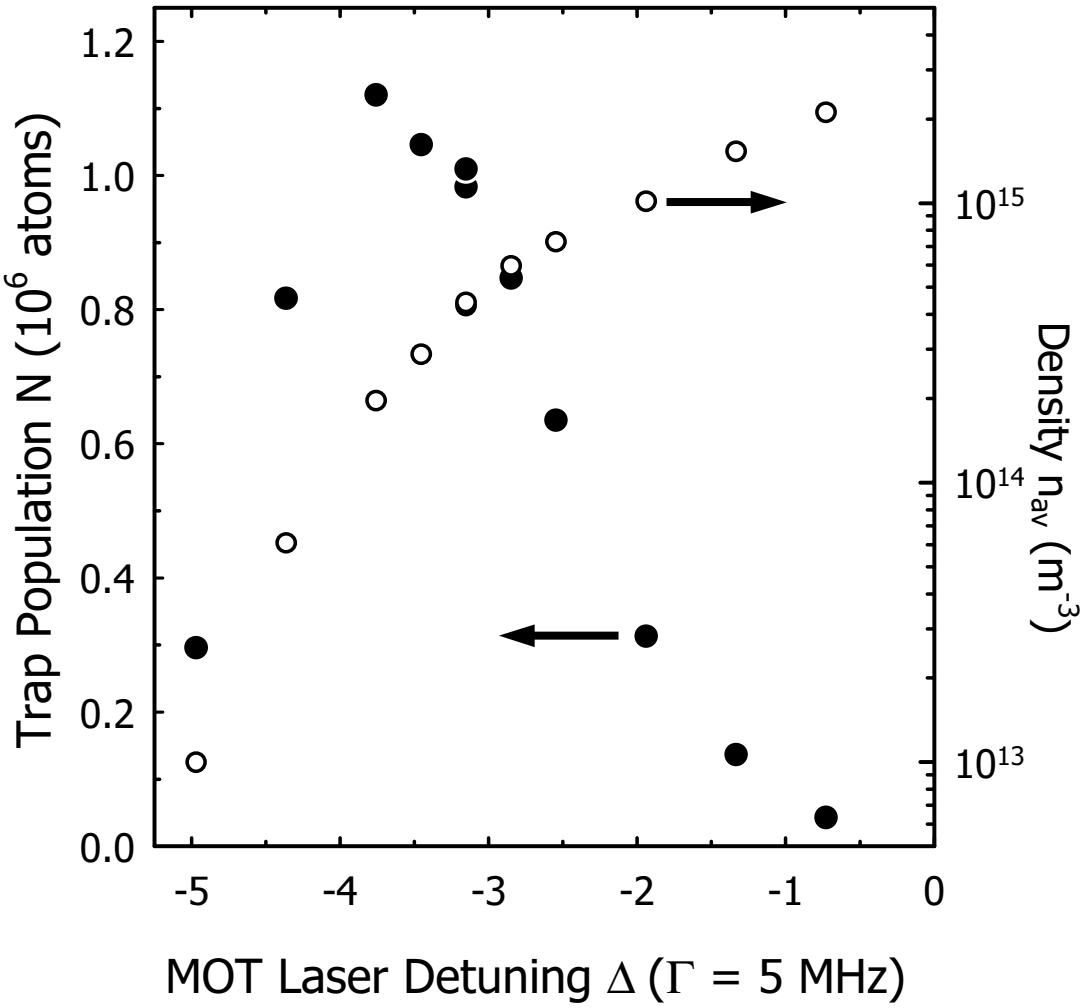

Figure 4. Trap population N (filled circles) and average density n_{av} (open circles) as a function of MOT laser detuning Δ, for a fixed total (six-beam) laser intensity of 0.65 mW/mm^2. Trap population values and density values have overall scale factor uncertainties of ±30 % and ±45 %, respectively, and random uncertainties of ±3 %.

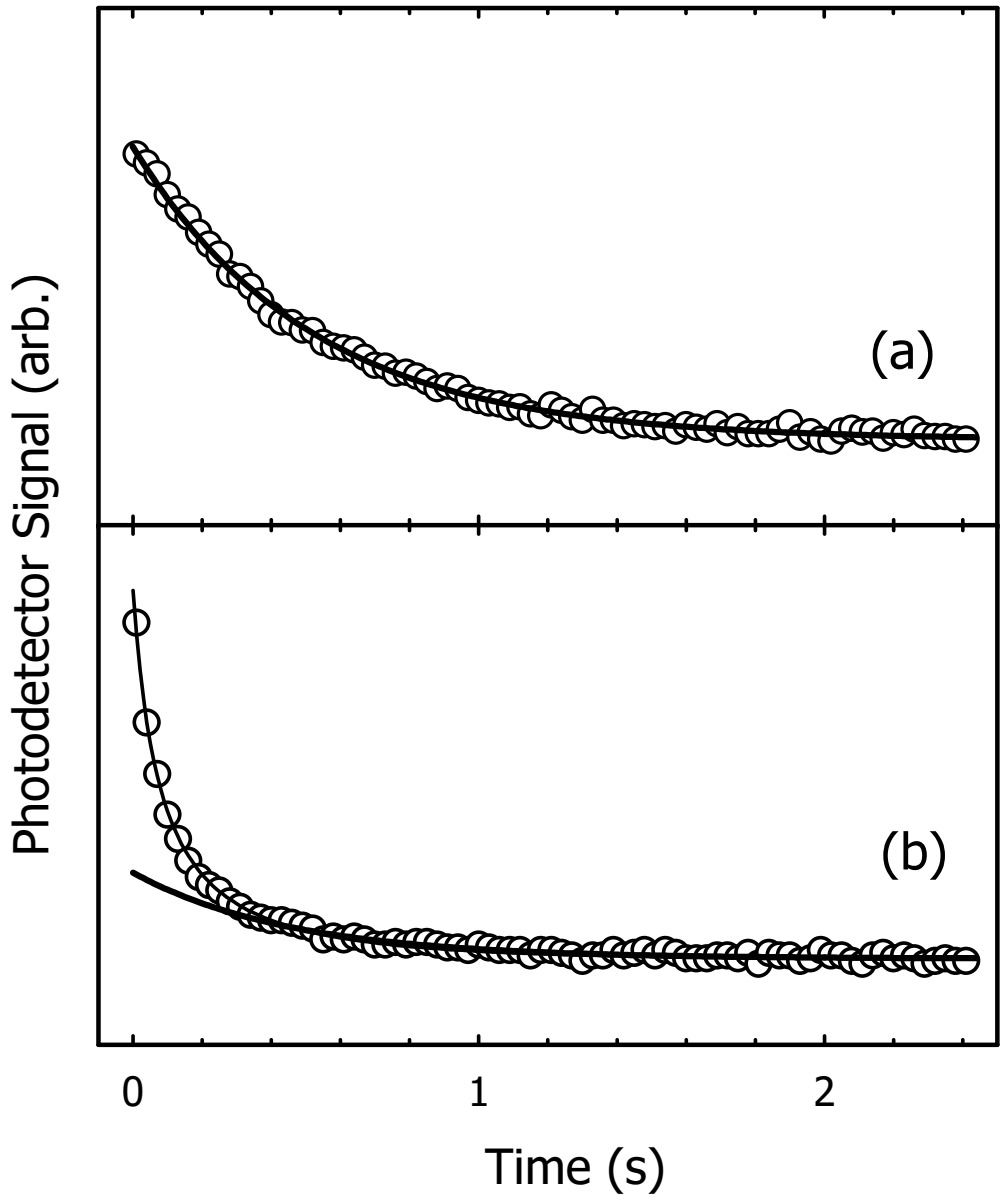

Figure 5. Observed MOT fluorescence decay curves for two different sets of trapping parameters. Each set of data points was obtained by averaging 8 MOT loading/decay cycles. The curves shown with the data are obtained either by fitting a simple decaying exponential to the data for times after 0.5 s (the heavy lines) or by fitting a non-exponential decay model to the data (the fine line). This model includes trap loss due to collisions between trapped atoms. Density dependence of the trap population decay is demonstrated by comparison of the data in (a) and (b). For (a) simple exponential decay was observed for an initial average density of 8×10^{12} m^{-3}, while in (b) the trapped sample had an initial average atom density of 3×10^{15} m^{-3}, and strongly non-exponential decay is evident.

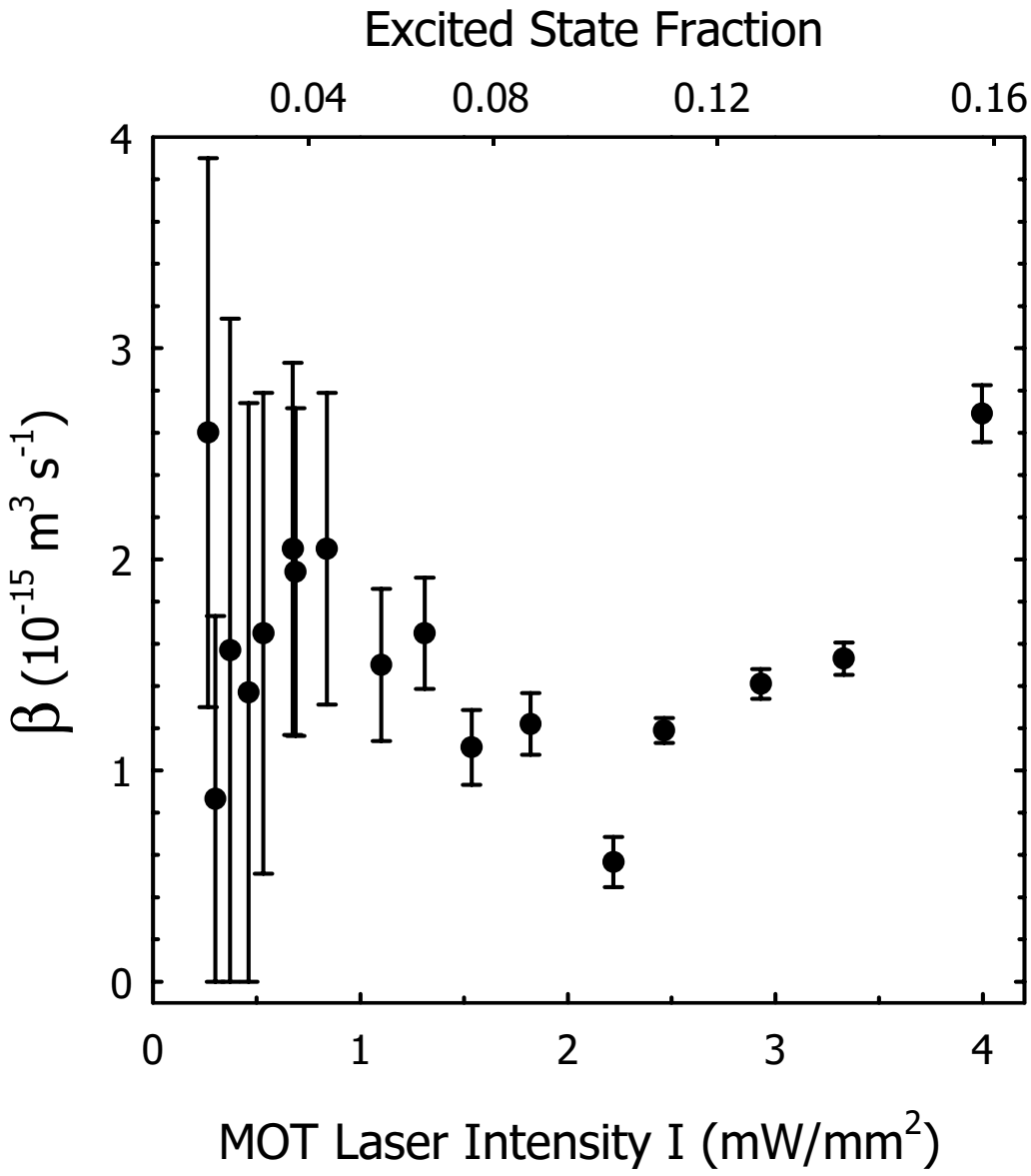

Figure 6. Density-dependent trap loss rate constant β as a function of total (six-beam) MOT laser intensity I, for a fixed laser detuning of –3.2 Γ (–16 MHz) from the atomic resonance, obtained from trap fluorescence decay curves. The top axis shows the effective excited state fraction for the given laser intensity and detuning. The vertical error bars indicate the range of β values that were obtained from fits to the decay curves, given the experimental uncertainty in the trap lifetime. In addition, there is an overall scale factor uncertainty of ±40 %.

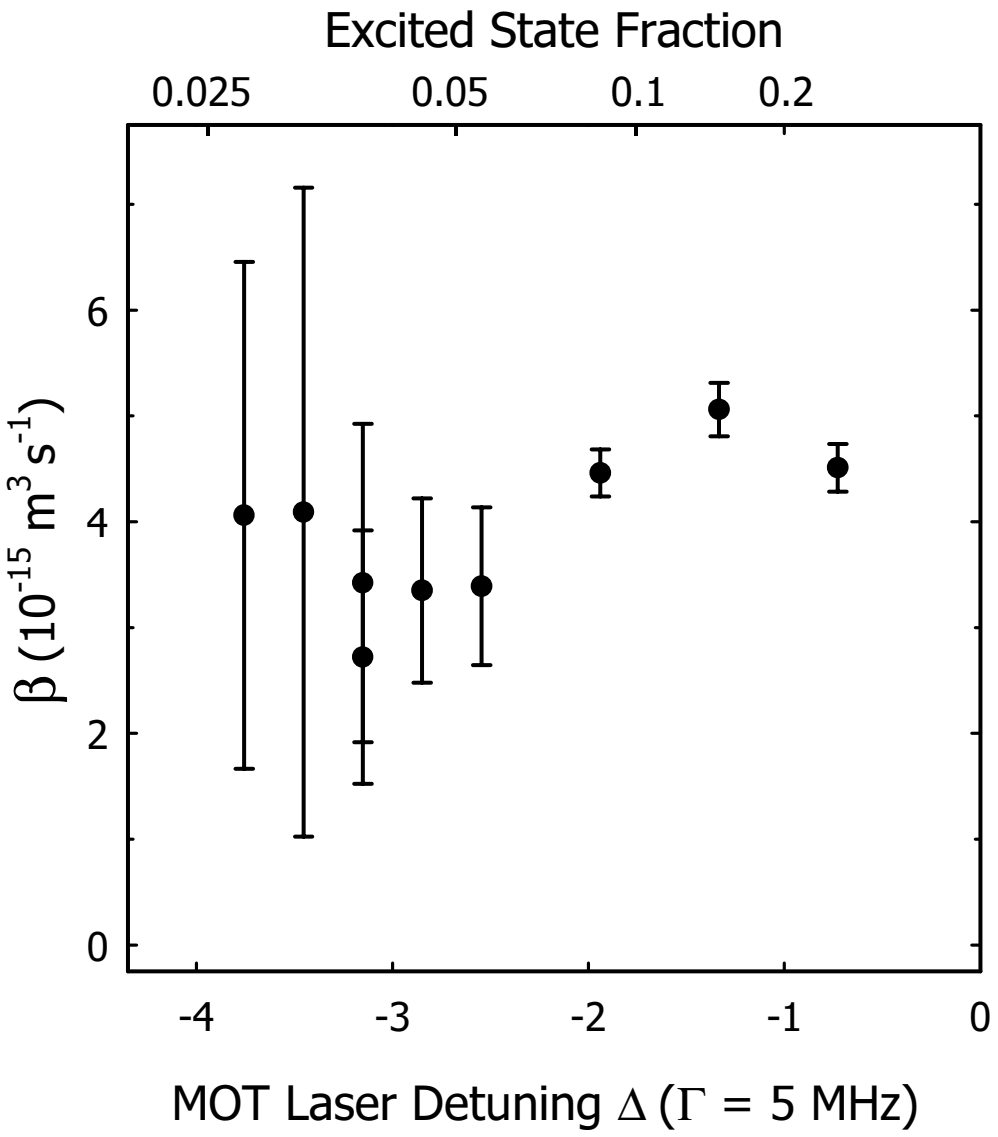

Figure 7. Density-dependent trap loss rate constant β as a function of MOT laser detuning Δ, for a fixed total (six-beam) laser intensity of 0.65 mW/mm^2, obtained from trap fluorescence decay curves. The top axis shows the effective excited state fraction for the given laser intensity and detuning. The vertical error bars indicate the range of β values that were obtained from fits to the decay curves, given the experimental uncertainty in the trap lifetime. In addition, there is an overall scale factor uncertainty of ±40 %.